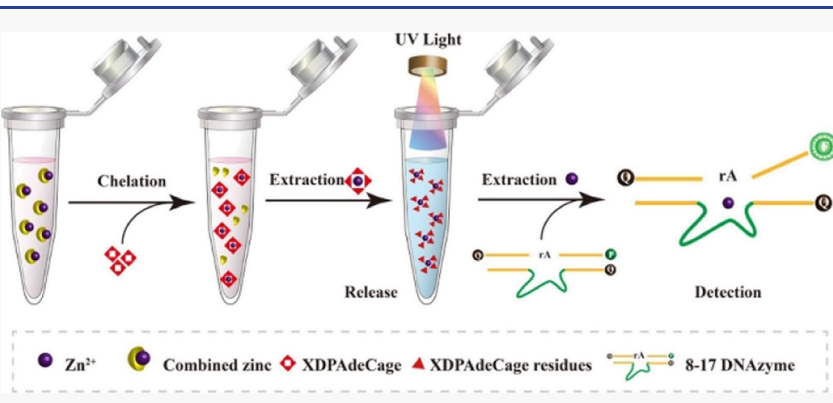


pubs.acs.org/ac Article

Detection and Quantification of Tightly Bound Zn²⁺ in Blood Serum Using a Photocaged Chelator and a DNAzyme Fluorescent Sensor

Shige Xing, Yao Lin, Liangyuan Cai, Prem N. Basa, Austin K. Shigemoto, Chengbin Zheng, Feng Zhang,* Shawn C. Burdette,* and Yi Lu*





ABSTRACT: DNAzymes have emerged as a powerful class of sensors for metal ions due to their high selectivity over a wide range of metal ions, allowing for on-site and real-time detection. Despite much progress made in this area, detecting and quantifying tightly bound metal ions, such as those in the blood serum, remain a challenge because the DNAzyme sensors reported so far can detect only mobile metal ions that are accessible to bind the DNAzymes. To overcome this major limitation, we report the use of a photocaged chelator, XDPAdeCage to extract the Zn²⁺ from the blood serum and then release the chelated Zn²⁺ into a buffer using 365 nm light for quantification by an 8–17 DNAzyme sensor. Protocols to chelate, uncage, extract, and detect metal ions in the serum have been developed and optimized. Because DNAzyme sensors for other metal ions have already been reported and more DNAzyme sensors can be obtained using in vitro selection, the method reported in this work will significantly expand the applications of the DNAzyme sensors from sensing metal ions that are not only free but also bound to other biomolecules in biological and environmental samples.

etal ions serve vital roles in biological systems; however, metal ions can also become biological toxins. Detecting and quantifying metal ions provide the opportunity to balance the beneficial and harmful impacts in living systems. To achieve this goal, inductively coupled plasma mass spectrometry (ICP-MS) has been used as a standard method. However, ICP-MS requires large and expensive equipment and a skilled operator. To overcome this limitation many sensors and imaging agents for metal ions have been developed,¹⁻⁶ among these DNAzymes have emerged as a promising new class of sensors.⁷⁻¹³ DNAzymes catalyze enzymatic reactions using DNA molecules. 14,15 DNAzymes often recruit metal ion cofactors to catalyze reactions efficiently. 16,17 We and others have used in vitro selection to select DNAzyme to catalyze phosphodiester transfer reactions from a DNA library of up to 10¹⁵ different sequences. 18,19 Using this approach, a number of DNAyzmes for different metal ions such as Zn²⁺, ^{20,21} Pb²⁺, ²² Na⁺, ¹⁹ Ag⁺, ²³ Cu²⁺, ²⁴ and Ca²⁺²⁵ have been developed. The DNAzymes have been converted into fluorescent, 24,26 colorimetric, 27,28 electrochemical, ^{23,29,30} or other types of sensors by conjugating either a fluorophore/quencher pair, gold nanoparticles, electrochemical, or other reporting groups to the DNAzyme. For example, we have reported a fluorescent DNAzyme sensor using a catalytic beacon, which has found wide applications in environmental monitoring, ^{31–33} medical diagnostics, ^{34,35} and imaging. ^{36–38}

s Supporting Information

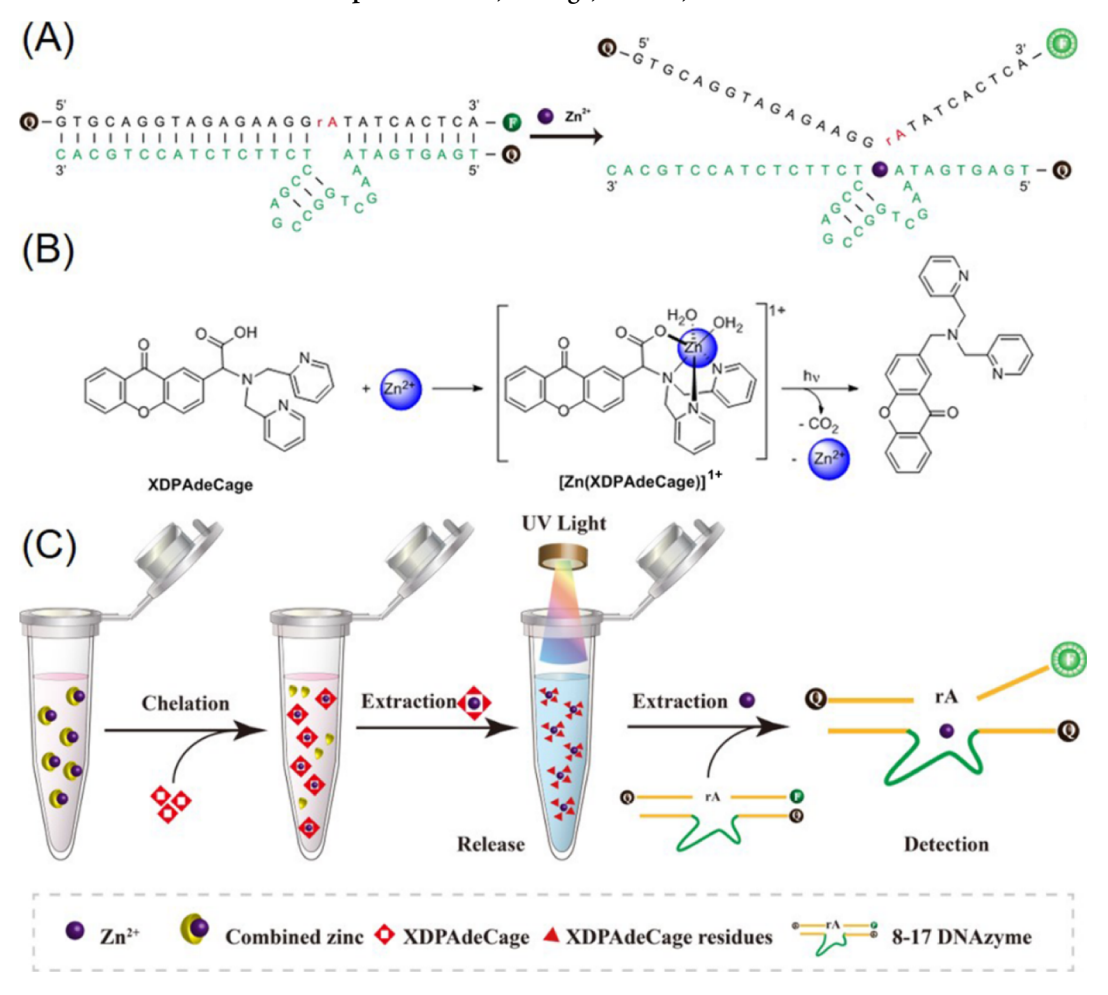
Despite numerous reports of DNAzyme-based sensors in detecting metal ions, sensing metal ions that are bound to biomolecules such as proteins and lipids remains a major obstacle because tightly bound metal ions are immobile and therefore inaccessible to DNAzyme sensors. While diagnostic

Received: January 12, 2021 Accepted: March 8, 2021 Published: March 31, 2021





Scheme 1. Schematic Illustration of the Steps to Chelate, Uncage, Extract, and Detect Metal Ions in Blood Serum^a



 a (A) 8–17 DNAzyme used in this work and the fluorescent sensor based on catalytic beacon; a fluorophore was conjugated to the 5' of the substrate strand and a DABCYL was conjugated to 3' of the substrate strand and 5' of the enzyme strand. In the absence of Zn^{2+} , the melting temperature of the two strands is above room temperature and thus hybridized, bringing the fluorophore and its quencher close to each other, resulting in a quenched fluorescent signal. In the presence of Zn^{2+} , the DNAzyme cleaves its substrate, resulting in lower melting temperature of the two strands and thus release of the cleaved product, making the fluorophore away from its quencher, and thus, an increase of fluorescent signal. (B) Schematic representing XDPAdeCage binding to Zn^{2+} and subsequent release by photolysis and resulting photoproducts. (C) Scheme to chelate and extract Zn^{2+} from BNCS using the XDPAdeCage chelator and then detection of Zn^{2+} using 8–17 DNAzyme.

tests have been developed for metal ions with relatively weak affinities for biomolecules (e.g., Ca^{2+} and Na^{+}), 39,40 similar tests for stronger affinity metal ions have not been effective. ⁴¹ Metal ions such as Zn^{2+} and Pb^{2+} often bind tightly ($K_{\text{d}} < 10$ nM) to many biomolecules that are significant components of the blood serum. The blood serum also contains endogenous molecules that exhibit colorimetric or fluorescent properties that can interfere with point-of-care tests that often rely on these signal transduction techniques.

We hypothesized that photoactive metal chelators that utilize a photodecarboxylation reaction to release Zn^{2+} may be able to circumvent the challenges to detecting tightly bound metal ions in the blood serum. If these photocages could extract the bound metal ions in the serum, we would be able to uncage the metal ions into aqueous solution free of the components in the serum that interfere with the quantification using DNAzyme sensors. We herein report that a recently developed Zn^{2+} photocaged chelator, Zn^{43} XDPAdeCage (2-(bis(pyridin-2-ylmethyl)amino)-2-(9-oxo-9*H*-xanthen-2-yl)-acetic acid, and xanthone dipicolylamine decarboxylation photocage) can chelate Zn^{2+} in the blood serum and then be

extracted as the $[Zn(XDPAdeCage)]^+$ complex. We have optimized protocols to separate the Zn^{2+} from the serum using XDPAdeCage, and then released the Zn^{2+} by uncaging the chelator with a 365 nm light. A 8–17 DNAzyme fluorescent sensor was then used to quantify the released Zn^{2+} . By combining photocages and DNAzyme sensors, the method demonstrated in this work may allow diagnostic tests for tightly bound metal ions that are difficult to detect using DNAzymes sensors.

■ EXPERIMENTAL SECTION

Chemicals and Apparatus. The XDPAdeCage chelator (see Scheme 1) was synthesized as described previously. ^{42,43} The substrate strand (/SFAM/-ACTCACTATrAGGAAGA-GATGGACGTG-/3BHQ/), and enzyme strand (CACGTC-CATCTCTCTCCGAGCCGGTCGAAATAGTGAGT-/3Dab/) of the 8–17 DNAzyme were synthesized by the IDT. 4-(2-Hydroxyethyl)-1-piperizineethanesulfonic acid (HEPES), tris(hydroxymethyl)aminomethane (Tris), sodium chloride (NaCl, 99.8%), zinc chloride (ZnCl₂,99.8%), dichloromethane

(CH₂Cl₂), methanol (CH₃OH), bovine newborn calf serum (BNCS), 4-(2-pyridylazo)resorcinol (PAR), and Triton X-114 were purchased from Fisher Scientific. Trace element serum L-2 RUO was purchased from Sero. Nitric acid (HNO₃ 65%) was purchased from Merck. The Zn²⁺ stock solution was prepared from ZnCl₂ using Millipore water. CH₃OH was routinely used as a co-solvent for preparing the stock solutions of the chelator. Photolysis was carried at 25 °C in a 1.0 cm quartz cuvette illuminated by 3 W UV light-emitting diode (LED) purchased from LED Engin (365 nm, 200 mW) powered by a 700 Ma LuxDriveFlexBox using a variable DC source set at 12 V DC.

Preparation of DNAzyme. To form the 8-17 DNAzyme, a mixture of the 20 nM substrate strand and 20 nM enzyme strand (50 mM Tris, 150 mM NaCl, pH = 7.4) was heated to and incubated at 95 °C for 5 min in a water bath and then allowed to cool to room temperature for 1 h. The resulting DNAzyme was stored in a 4 °C.

Measurements. Fluorescence measurements were conducted on a HORIBA fluorescence spectrophotometer (Fluro Max-P). In a typical experiment, 100 μ L of DNAzyme and 100 μ L of the extracted sample were sequentially added into a tube and measured immediately by a fluorescence spectrophotometer. Ultraviolet-visible (UV-vis) absorption spectra were obtained by taking sample solutions in a 1.0 cm quartz cuvette at 25 °C with total volumes kept at 100 μ L and recorded on an Agilent Technologies, Cary 8454 UV-vis spectrometer. ICP-MS (NexION300Q, PE) was employed as a standard method to verify the quantities of zinc recovered from the standard metal solutions and the serum samples. Trace elements serum was used as a quality control material to monitor precision and trueness of laboratory measurement procedures. All samples were digested and dissolved with HNO3 before analysis and measured in triplicate.

■ RESULTS AND DISCUSSION

General Procedures to Chelate, Extract, and Detect Metal lons in the Serum. The photocaged XDPAdeCage chelator can bind and release Zn²⁺ upon exposure to light. We therefore hypothesized that XDPAdeCage could remove Zn²⁺ from other ligating species in serum samples and then release the metal ion for further analysis. After using XDPAdeCage to extract bound Zn²⁺ in the serum, the resulting [Zn-(XDPAdeCage)]+ complex is separated by extraction into CH₂Cl₂ (Scheme 1). Upon the removal of the organic solvent, the isolated [Zn(XDPAdeCage)]+ is then redissolved in the CH₃OH/H₂O solution, 42,43 and the Zn²⁺ is released by photolysis with 365 nm light. This process efficiently removes Zn²⁺ from the serum for further analysis. Because the XDPAdeCage photoproducts could interfere with the DNAzyme sensing, the organic products were removed by reconstitution with water and extraction with CH2Cl2. After the separation of layers, this provides aqueous solution of Zn²⁺ that can be quantified using the 8-17 DNAzyme fluorescent

Chelation of Zn^{2+} by the XDPAdeCage Ligand. The Zn^{2+} -binding affinity of XDPAdeCage was measured using a competitive ligand binding assay with PAR. ^{42,43} Because the binding affinity of $[Zn(XDPAdeCage)]^+$ ($K_d = 4.6 \pm 0.8 \text{ pM}$) is weaker than that of $[Zn(PAR)_2]$ ($K_d = 0.5 \text{ pM}$), we employed similar assays to investigate the feasibility of the assay outlined in Scheme 1. We used PAR as a surrogate for the Zn^{2+} -binding ligands in the serum to determine the optimal

conditions needed to extract bound Zn^{2+} in point-of-care samples. This strategy provides a convenient spectroscopic technique to quantify extracted Zn^{2+} because the spectroscopic properties of XDPAdeCage do not change significantly upon Zn^{2+} binding, whereas $[Zn(PAR)_2]$ and apo-PAR are easily distinguishable by UV–vis spectroscopy. The absorption intensity of PAR and $[Zn(PAR)_2]$ was found to be 0.2–1.0 when the concentration of PAR was 26 μ M, which was the optimal absorption intensity for the UV–vis analysis. Therefore, 26 μ M of PAR was chosen for the investigations.

To determine the amount of XDPAdeCage necessary to efficiently extract Zn^{2+} , different ratios of XDPAdeCage and Zn^{2+} were incubated for 60 min to establish the binding equilibrium, before 26 μ M PAR (40 mM HEPES, 100 mM KCl, pH = 7.5) was added into the solutions. The UV-vis spectrum of PAR which has an λ_{max} at 415 nm and $[Zn(PAR)_2]$ which has an λ_{max} at 500 nm can be measured simultaneously to determine the speciation of Zn^{2+} with respect to [XDPAdeCage] (Figure 1A). The intensity of the

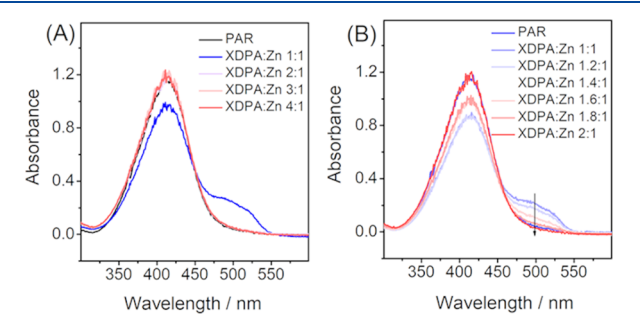


Figure 1. UV—vis spectra of the PAR solution $[Zn(XDPAdeCage)]^+$ after the formation of $[Zn(XDPAdeCage)]^+$ with different ratios. Large ratio (A) and narrow ratio (B) of XDPAdeCage and Zn^{2+} . The composite results suggest that a 2:1 ratio of XDPAdeCage to total Zn^{2+} present is necessary for complete extraction.

PAR peak at 415 nm indicates the amount of Zn²⁺ successfully extracted from [Zn(PAR)₂] by XDPAdeCage. The residual absorbance at 500 nm with XDPAdeCage and Zn²⁺ in a 1:1 ratio suggests that Zn²⁺ has not been removed completely from [Zn(PAR)₂] by the XDPAdeCage ligand. As the XDPAde-Cage/Zn²⁺ ratio was increased from 2:1 to 3:1 and 4:1, the 500 nm band disappeared, which suggests that XDPAdeCage completely sequesters all the Zn²⁺ ratios of 2:1 and higher. The optimal ratio of XDPAdeCage/Zn²⁺ between 1:1 and 2:1 was determined by additional measurements. As shown in Figure 1B, the absorption of the [Zn(PAR)₂] complex at 500 nm decreases gradually as the ratio approaches 2:1 with a concomitant increase in the apo-PAR band at 415 nm. These results suggest that a 2-fold excess of XDPAdeCage to the approximate amount of bound Zn²⁺ contained in a serum sample will maximize the extraction efficiency.

After determining the optimal ratios of XDPAdeCage necessary to extract Zn²⁺, we varied the chelation time and found 40 min with stirring to be optimal (see Figure S1). In addition, because the [Zn(XDPAdeCage)]⁺ complex is soluble in CH₂Cl₂, we changed the percentages of a surfactant Triton X-114 (Figure S2A) and NaCl (Figure S2B), extraction time (Figure S2C), and the percentages of CH₃OH (Figure S2D) and found no obvious benefit from the Triton X-114, 10 mM NaCl, 60 min extraction time, and 10% CH₃OH in aqueous buffer to allow for the maximal extraction efficiency.

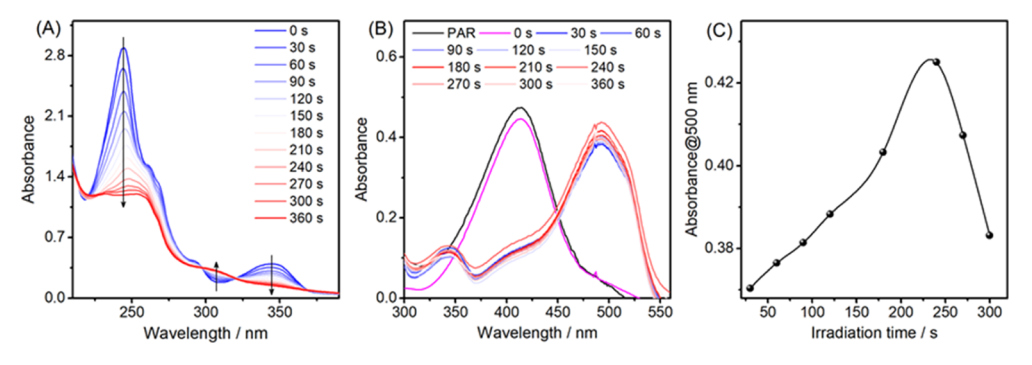


Figure 2. (A) UV–vis spectrum changes of $100~\mu M~[Zn(XDPAdeCage)]^+$ in water at different irradiation times. Irradiation at 365 nm (LED, 3 W cm⁻²) leads to the erosion of the absorption band at 245 and 345 nm associated with the photocaged compound, and the concurrent formation of a band at a 310 nm characteristic of the photoproduct. (B) UV–vis spectrum of PAR in aqueous solution titrated with the $[Zn(XDPAdeCage)]^+$ complex with different irradiation times. (C) Photolysis of the $[Zn(XDPAdeCage)]^+$ complex as monitored by UV–vis absorbance changes (λ = 500 nm) through adding PAR solution.

Table 1. Performance of Zn²⁺ Detection in the Blood Serum Based on XDPAdeCage

		chelation		photolysis	
spiked Zn ²⁺ (μ M)	total Zn^{2+} in samples $(\mu\mathrm{M})$	Zn^{2+} extracted by XDPAdeCage (μM)	chelation Efficiency (%) ^a	released Zn ²⁺ (μ M)	total Zn ²⁺ recovery (%) ^a
10	12.1 ± 0.1	9.1 ± 2.3	75.2	3.4 ± 1.4	28.1
20	21.4 ± 0.6	15.8 ± 3.3	73.8	6.8 ± 3.5	31.8
40	41.3 ± 0.2	31.3 ± 2.8	75.8	11.8 ± 3.0	28.6
80	80.9 ± 5.0	58.2 ± 9.3	71.9	21.1 ± 6.9	26.1
160	161.1 ± 1.9	119.7 ± 8.0	74.3	46.5 ± 19.1	28.9

^aCompared with the concentration of total zinc in samples.

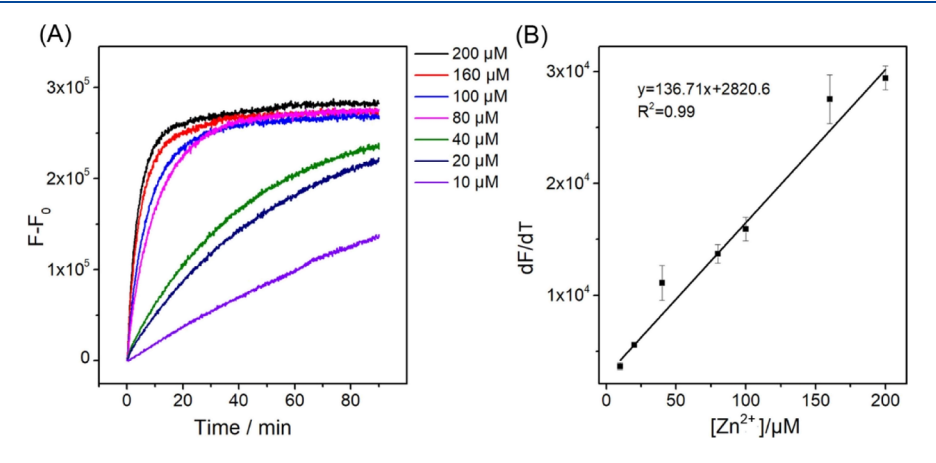


Figure 3. (A) Obtained DNAzyme sensor's fluorescent signal over time after chelation, extraction, and photolysis of the blood serum spiked with different concentrations of Zn^{2+} . (B) Corresponding calibration curve of the slope of kinetic curves (1–10 min) vs the concentration of Zn^{2+} . The error bars represent the SD calculated from three independent experiments.

Optimization of Photolysis Time. The optimal irradiation time of the uncaging of [Zn(XDPAdeCage)]⁺ was determined by irradiating with 365 nm light (3 W cm⁻²) and monitoring changes in the UV—vis absorbance spectrum. As shown in Figure 2A, the irradiation of [Zn(XDPAdeCage)]⁺ in the 10% CH₃OH solution results in the rapid erosion of the absorption bands at 245 and 345 nm, which is characteristic of [Zn(XDPAdeCage)]⁺ uncaging. Concurrently, an absorption band at 310 nm forms, which is attributed to photolysis products. At irradiation times longer than 240 s, minimal changes in the spectrum are observed. PAR was added to the fresh solution, and the photolysis was repeated to provide supporting evidence for an optimal photolysis time. As the irradiation time increases from 0 to 300 s, the free PAR absorption band at 415 nm decreases, while the [Zn(PAR)₂]

absorption band at 500 nm increases (Figure 2B). A plot of the absorption at 500 nm versus irradiation time indicates that more Zn^{2+} is released as photolysis time increase (Figure 2C). Since evidence suggested that the photolysis was complete, 240 s was chosen as the optimal irradiation time.

Analytical Performance of the Assay. Based on the results from the above optimization steps, we investigated measuring Zn^{2+} in the blood serum using the optimized experimental conditions for coupling XDPAdeCage extraction and DNAzyme sensing. First, we spiked serum samples with different Zn^{2+} between $10-60~\mu M$ and used XDPAdeCage to extract the Zn^{2+} for analysis. While dissolving in CH_2Cl_2 , the Zn^{2+} extracted into the organic layer as $[Zn(XDPAdeCage)]^+$ was quantified by ICP-MS (Table 1). When being divided by the total Zn^{2+} in the samples before chelation, the chelation

efficiency was consistently around 74%. After photolysis, the released $\mathrm{Zn^{2+}}$ in aqueous solution was measured by ICP–MS; when compared with the total $\mathrm{Zn^{2+}}$ in the sample, the total $\mathrm{Zn^{2+}}$ recovery from both chelation and photolysis is around 30% (Table 1). Both the chelation efficiency and total $\mathrm{Zn^{2+}}$ recovery are consistent with those in our previous report. ⁴³

We repeated the Zn²⁺ measurements using the DNAzyme sensor fluorescence instead of ICP-MS. The XDPAdeCage was added to a 1 mL serum sample spiked with different Zn² concentrations, and the above extraction protocols were used before Zn²⁺ quantification by combing 100 μ L each of the DNAzyme sensor solution and extracted sample solution. As shown in Figure 3A, the fluorescence intensity increases over time upon the addition of the photolyzed serum extract. Furthermore, at higher Zn²⁺ concentrations, the emission intensity increases more rapidly relative to lower concentrations. The slope of these kinetic curves from 1 to 10 min fits a linear model because the slope at the early time points is less susceptible to interference from the background fluorescence attributed to other emissive serum species. The corresponding calibration curve of the rates of the cleavage versus the concentration of Zn²⁺ is shown in Figure 3B, and the detection limit is found to be 2.96 μ M Zn²⁺ based on the 3σ /slope calculation. The reproducibility of these methods over five measurements at 100 μ M Zn²⁺ was 5.6% of the relative standard deviation (SD). The actual extracted Zn2+ is finally determined by a calibration curve obtained by adding a series concentration of Zn2+ after the blank serum was treated with chelation and photolysis steps, as shown in Figure S3A and B.

To verify the accuracy of the photocage/DNAzyme sensor method, ICP-MS was also used to measure Zn $^{2+}$ in the same photolyzed samples. As shown in Table 2, the Zn $^{2+}$ in different

Table 2. Results for Zn²⁺ in BNCS by the DNAzyme Fluorescent Sensor and ICP-MS Detection

sample	DNAzyme sensor (μM)	ICP-MS (μM)
1	2.7 ± 0.5	3.4 ± 1.4
2	5.6 ± 0.1	6.8 ± 3.5
3	11.5 ± 2.2	11.8 ± 3.0
4	18.9 ± 1.4	21.1 ± 6.9
5	22.6 ± 1.7	26.0 ± 2.0
6	41.7 ± 3.6	46.5 ± 19.1
7	44.2 ± 2.7	48.2 ± 11.6

samples determined by the DNAzyme sensor correlate well with those determined by ICP–MS with a Pearson correlation between the DNAzyme sensor and ICP–MS of 0.92. Therefore, our method of measuring Zn²⁺ in the serum using a photocaged chelator and a DNAzyme fluorescent sensor is comparable to ICP–MS.

CONCLUSIONS

In conclusion, we have developed a novel photocaged chelator-based strategy to allow a DNAzyme sensor to measure the $\mathrm{Zn^{2+}}$ concentrations in serum samples. After photolysis and extraction, the $\mathrm{Zn^{2+}}$ that are bound tightly to biomolecules in the serum can be released into aqueous solution as a free metal ion that can be measured by the DNAzyme fluorescent sensor, with minimal interfering species from the serum. Because a small portable fluorometer has been developed and commercially available for DNAzyme-based detection, the method demonstrated in this work may allow for a more convenient

and cost-effective quantification of metal ions than ICP-MS. Because DNAzyme sensors for other metal ions have already been reported and more DNAzyme sensors can be obtained using in vitro selection, the method reported in this work will significantly expand the applications of the DNAzyme sensors from sensing metal ions that are not only free but also bound to other biomolecules in biological and environmental samples.

ASSOCIATED CONTENT

Supporting Information

The Supporting Information is available free of charge at https://pubs.acs.org/doi/10.1021/acs.analchem.1c00140.

Experimental details and more discussion for the optimization of chelation time, liquid–liquid extraction, concentration of NaCl, extraction time, concentration of CH₃OH, and calibration curve obtained by blank solution (PDF)

AUTHOR INFORMATION

Corresponding Authors

Feng Zhang — Institute of Food Safety, Chinese Academy of Inspection & Quarantine, Beijing 100176, China; orcid.org/0000-0002-7888-9669; Email: fengzhang@126.com

Shawn C. Burdette — Department of Chemistry and Biochemistry, Worcester Polytechnic Institute, Worcester, Massachusetts 01609-2280, United States; orcid.org/0000-0002-2176-0776; Email: scburdette@wpi.edu

Yi Lu — Department of Chemistry, Department of Biochemistry, University of Illinois at Urbana-Champaign, Urbana, Illinois 61801, United States; orcid.org/0000-0003-1221-6709; Email: yi-lu@illinois.edu

Authors

Shige Xing — Department of Chemistry, Department of Biochemistry, University of Illinois at Urbana-Champaign, Urbana, Illinois 61801, United States; Institute of Food Safety, Chinese Academy of Inspection & Quarantine, Beijing 100176, China

Yao Lin – Department of Chemistry, Department of Biochemistry, University of Illinois at Urbana-Champaign, Urbana, Illinois 61801, United States; Department of Forensic Analytical Toxicology, West China School of Basic Medical Sciences & Forensic Medicine, Sichuan University, Chengdu, Sichuan 610041, China

Liangyuan Cai — Department of Chemistry, Department of Biochemistry, University of Illinois at Urbana-Champaign, Urbana, Illinois 61801, United States

Prem N. Basa – Department of Chemistry and Biochemistry, Worcester Polytechnic Institute, Worcester, Massachusetts 01609-2280, United States

Austin K. Shigemoto – Department of Chemistry and Biochemistry, Worcester Polytechnic Institute, Worcester, Massachusetts 01609-2280, United States

Chengbin Zheng – Key Laboratory of Green Chemistry and Technology, Ministry of Education, College of Chemistry, Sichuan University, Chengdu, Sichuan 610064, China

Complete contact information is available at: https://pubs.acs.org/10.1021/acs.analchem.1c00140

Author Contributions

S.X. and Y. Lin contributed equally to this work. Y. Lin, C.Z., F.Z., S.X., and Y. Lu designed the experiments, S.C.B. and P.N.B. and A.K.S. designed and synthesized the photocaged chelator. S.X., Y. Lin, and L.C. carried out extraction, detection, and evaluation of the performance of the system, with S.X. and Y. Lin contributing equally. The manuscript was written through contributions of all the authors. All the authors have given approval to the final version of the manuscript.

Notes

The authors declare the following competing financial interest(s): Y. Lu is a co-Founder of ANDalyze, Inc. and GlucoSentient, Inc.

ACKNOWLEDGMENTS

The work described in this article is supported by the U.S. National Institutes of Health (GM124316), Y.L. and L.Y.C. Acknowledge the financial support from the China Scholarship Council (CSC). S.C. Burdette acknowledges support from NSF CHE-2004088. We thank Dr. Zhenglin Yang, Dr. Ryan J. Lake, and Dr. Muyi He for their helpful suggestions and support.

REFERENCES

- (1) Rupcich, N.; Chiuman, W.; Nutiu, R.; Mei, S.; Flora, K. K.; Li, Y.; Brennan, J. D. *J. Am. Chem. Soc.* **2006**, *128*, 780–790.
- (2) Domaille, D. W.; Que, E. L.; Chang, C. J. Nat. Chem. Biol. 2008, 4, 168–175.
- (3) Qian, F.; Zhang, C.; Zhang, Y.; He, W.; Gao, X.; Hu, P.; Guo, Z. J. Am. Chem. Soc. **2009**, 131, 1460–1468.
- (4) Yang, C.; Yin, X.; Huan, S.-Y.; Chen, L.; Hu, X.-X.; Xiong, M.-Y.; Chen, K.; Zhang, X.-B. *Anal. Chem.* **2018**, *90*, 3118–3123.
- (5) Li, L.; Xing, H.; Zhang, J.; Lu, Y. Acc. Chem. Res. 2019, 52, 2415–2426.
- (6) Fan, Y.; Xing, H.; Xue, Y.; Peng, C.; Li, J.; Wang, E. Anal. Chem. **2020**, 92, 16066–16071.
- (7) Tang, Y.; Ge, B.; Sen, D.; Yu, H.-Z. Chem. Soc. Rev. 2014, 43, 518-529.
- (8) Gong, L.; Zhao, Z.; Lv, Y.-F.; Huan, S.-Y.; Fu, T.; Zhang, X.-B.; Shen, G.-L.; Yu, R.-Q. Chem. Commun. 2015, 51, 979-995.
- (9) Cui, L.; Peng, R.; Fu, T.; Zhang, X.; Wu, C.; Chen, H.; Liang, H.; Yang, C. J.; Tan, W. Anal. Chem. **2016**, 88, 1850–1855.
- (10) Zhou, W.; Saran, R.; Liu, J. Chem. Rev. 2017, 117, 8272-8325.
- (11) Liu, M.; Chang, D.; Li, Y. Acc. Chem. Res. 2017, 50, 2273-
- (12) Lake, R. J.; Yang, Z.; Zhang, J.; Lu, Y. Acc. Chem. Res. 2019, 52, 3275–3286.
- (13) Liu, R.; McConnell, E. M.; Li, J.; Li, Y. J. Mater. Chem. B 2020, 8, 3213–3230.
- (14) Liu, M.; Zhang, Q.; Kannan, B.; Botton, G. A.; Yang, J.; Soleymani, L.; Brennan, J. D.; Li, Y. *Angew. Chem., Int. Ed.* **2018**, *57*, 12440–12443.
- (15) Ma, L.; Liu, J. iScience 2020, 23, 100815.
- (16) Peng, H.; Li, X.-F.; Zhang, H.; Le, X. C. Nat. Commun. 2017, 8, 14378.
- (17) Fan, H.; Bai, H.; Liu, Q.; Xing, H.; Zhang, X.-B.; Tan, W. Anal. Chem. 2019, 91, 13143–13151.
- (18) Breaker, R. R.; Joyce, G. F. Cell Chem. Biol. 1994, 1, 223-229.
- (19) Torabi, S.-F.; Wu, P.; McGhee, C. E.; Chen, L.; Hwang, K.; Zheng, N.; Cheng, J.; Lu, Y. Proc. Natl. Acad. Sci. U.S.A. 2015, 112, 5903–5908.
- (20) Mazumdar, D.; Nagraj, N.; Kim, H.-K.; Meng, X.; Brown, A. K.; Sun, Q.; Li, W.; Lu, Y. J. Am. Chem. Soc. 2009, 131, 5506-5515.
- (21) Moon, W. J.; Yang, Y.; Liu, J. ChemBioChem 2021, 22, 779–789
- (22) Li, J.; Lu, Y. J. Am. Chem. Soc. 2000, 122, 10466-10467.

- (23) Saran, R.; Liu, J. Anal. Chem. 2016, 88, 4014-4020.
- (24) Liu, J.; Lu, Y. J. Am. Chem. Soc. 2007, 129, 9838-9839.
- (25) Zhou, W.; Saran, R.; Huang, P.-J. J.; Ding, J.; Liu, J. ChemBioChem 2017, 18, 518-522.
- (26) Mei, S. H. J.; Liu, Z.; Brennan, J. D.; Li, Y. J. Am. Chem. Soc. **2003**, 125, 412–420.
- (27) Liu, J.; Lu, Y. J. Am. Chem. Soc. 2003, 125, 6642-6643.
- (28) Manochehry, S.; McConnell, E. M.; Tram, K. Q.; Macri, J.; Li, Y. Front. Chem. 2018, 6, 332.
- (29) Shen, L.; Chen, Z.; Li, Y.; He, S.; Xie, S.; Xu, X.; Liang, Z.; Meng, X.; Li, Q.; Zhu, Z.; Li, M.; Le, X. C.; Shao, Y. *Anal. Chem.* **2008**, *80*, 6323–6328.
- (30) Wang, H.; Liu, Y.; Wang, J.; Xiong, B.; Hou, X. Microchim. Acta **2020**, 187, 207.
- (31) McGhee, C. E.; Loh, K. Y.; Lu, Y. Curr. Opin. Biotechnol. 2017, 45, 191-201.
- (32) Peng, D.; Li, Y.; Huang, Z.; Liang, R.-P.; Qiu, J.-D.; Liu, J. Anal. Chem. **2019**, 91, 11403–11408.
- (33) Feng, M.; Gu, C.; Sun, Y.; Zhang, S.; Tong, A.; Xiang, Y. Anal. Chem. **2019**, *91*, 6608–6615.
- (34) Zhang, J.; Lu, Y. Angew. Chem., Int. Ed. **2018**, 57, 9702–9706.
- (35) Xiong, Y.; Zhang, J.; Yang, Z.; Mou, Q.; Ma, Y.; Xiong, Y.; Lu, Y. J. Am. Chem. Soc. 2020, 142, 207–213.
- (36) Lin, Y.; Yang, Z.; Lake, R. J.; Zheng, C.; Lu, Y. Angew. Chem., Int. Ed. 2019, 58, 17061–17067.
- (37) Xiong, M.; Yang, Z.; Lake, R. J.; Li, J.; Hong, S.; Fan, H.; Zhang, X. B.; Lu, Y. Angew. Chem., Int. Ed. 2020, 132, 1907–1912.
- (38) Samanta, D.; Ebrahimi, S. B.; Mirkin, C. A. Adv. Mater. 2020, 32, 1901743.
- (39) Liu, J.; Lu, Y. Adv. Mater. 2006, 18, 1667-1671.
- (40) Mirzazadeh, M.; Morovat, A.; James, T.; Smith, I.; Kirby, J.; Shine, B. *Emerg. Med. J.* **2016**, 33, 181–186.
- (41) Ali, M.; Kumar, A.; Kumar, M.; Pandey, B. N. Biochimie 2016, 123, 117-129.
- (42) Basa, P. N.; Antala, S.; Dempski, R. E.; Burdette, S. C. Angew. Chem., Int. Ed. 2015, 54, 13027-13031.
- (43) Basa, P. N.; Barr, C. A.; Oakley, K. M.; Liang, X.; Burdette, S. C. J. Am. Chem. Soc. **2019**, 141, 12100–12108.
- (44) Schlosser, K.; Li, Y. ChemBioChem 2010, 11, 866-879.
- (45) Yang, Z.; Loh, K. Y.; Chu, Y.-T.; Feng, R.; Satyavolu, N. S. R.; Xiong, M.; Nakamata Huynh, S. M.; Hwang, K.; Li, L.; Xing, H.; Zhang, X.; Chemla, Y. R.; Gruebele, M.; Lu, Y. J. Am. Chem. Soc. 2018, 140, 17656–17665.
- (46) Kochańczyk, T.; Jakimowicz, P.; Krężel, A. Chem. Commun. 2013, 49, 1312–1314.